

MODELLING AND DESIGN FOR PM/EM MAGNETIC BEARINGS

D. Pang, J. A. Kirk, D. K. Anand, R. G. Johnson

**Department of Mechanical Engineering
University of Maryland, College Park, MD 20742, U. S. A.**

R. B. Zmood

**Department of Communication and Electrical Engineering
Royal Melbourne Institute of Technology, Melbourne, Victoria 3000, Australia**

SUMMARY

This paper presents a mathematical model of a permanent magnet/electromagnet [PM/EM] radially active bearing. The bearing is represented by both a reluctance model and a stiffness model. The reluctance model analyzes the magnetic circuit of the PM/EM bearing. The stiffness model uses force equilibrium equations to present the behavior of the bearing. By combining the two models the performance of the bearing can be predicted given geometric dimensions, permanent magnet strength, and the parameters of the EM coils.

The overall bearing design including the PM and EM design is subject to the performance requirement and physical constraints. A study of these requirements and constraints is discussed. The PM design is based on the required magnetic flux for proper geometric dimensions and magnet strength. The EM design is based on the stability and force slew rate consideration, and dictates the number of turns for the EM coils and the voltage and current of the power amplifier. An overall PM/EM bearing design methodology is proposed and a case study is also demonstrated.

INTRODUCTION

A magnetic bearing design combining permanent magnets and electromagnetic coils has the advantages of compact size, high efficiency and low heat generation. Permanent magnets containing mainly rare earth material have a high energy density and contribute the major magnetic flux in the bearing. The electromagnetic coils offer the additional magnetic flux to enhance the desired performance of the bearing. This design can decrease the size of the bearing, reduce the power consumption, and generate less heat in the bearing. There are various PM/EM bearing designs; this paper will discuss the PM/EM bearing developed in the University of Maryland for a flywheel energy storage system [1].

The PM/EM magnetic bearing shown Figure 1 is a passive axial support and radial active control design. The permanent magnets generate a bias flux across the air gap and support the axial load but create a destabilized force in the radial direction if the flywheel is not centered. A feedback control system senses the position of the flywheel and sends the appropriate control current into the EM coils. This generates the necessary corrective force to stabilize the system. The bearing's function is to magnetically suspend and center a rotating flywheel that can store kinetic energy.

The mathematical model of the PM/EM bearing can be represented by both a reluctance model and a stiffness model. The former applies the magnetic circuit theory and geometric dimensions of the bearing to analyze the magnetic flux in the air gap. The latter evaluates stiffness equations and force equilibrium equations to present the behavior of the bearing. By combining both models the bearing performance can be predicted and designed. There are some physical restrictions for the

mathematical model such as magnetic saturation, size limitation and electrical constraints that will be discussed later.

RELUCTANCE MODEL

In Figure 2 there is a typical hysteresis loop for the permanent magnetic material [2]. The permanent magnet inherits a flux density B_r , remanence, at zero magnetizing force. If a negative magnetizing force is applied to the magnet until the flux density reduces to zero, that magnetizing force is called the coercive force H_c . For most applications the permanent magnet operates in the second quadrant of the B-H curve between B_r and H_c . The slope of the B-H curve (the ratio of B to H) is denoted the permeability. The most commonly used permeability is the recoil permeability μ_r , which is the slope of the minor hysteresis loop. It is approximately equal to the slope of the B-H curve at zero magnetizing force and is usually presented as a relative value to the permeability of the air.

For an ideal permanent magnet having a strong intrinsic coercive force the B-H curve is a straight line between B_r and H_c shown in Figure 3. The minor hysteresis loop will follow the B-H curve and the recoil permeability is the ratio of B_r and H_c . The equation for the B-H curve is

$$B_m = \mu_0 \mu_r H_m + B_r \quad (1)$$

In a static magnetic field condition, magnetic circuit theory is used to analyze the magnetic flux by solving an equivalent electrical circuit. The reluctance of a magnetic flux path, which is analogous to an electrical resistance, is a function of its length L , cross section area A and permeability μ ,

$$R = L/(\mu A) \quad (2)$$

The permanent magnet can be simulated as a battery of voltage $B_r A_m R_m$ with an internal resistance R_m or a current source $H_m L_m$ with a shunt reluctance R_m [3]. The EM coils can be treated as voltage sources of quantity NI .

Figure 4(a) shows a magnetic circuit containing a permanent magnet, a core material of high (assumed infinite) permeability and an electromagnetic coil. There is a magnetic flux generated by the permanent magnet and the EM coil. When the magnetic flux passes through the air gap, it is separated into two paths: one is the air gap flux path directly across the pole faces and the other is a leakage flux path around the air gap flux path. The reluctance of the air gap and the leakage path are R_g and R_L . The total reluctance R_T is the combination of both reluctances. The equivalent electrical circuit can be plotted as Figure 4(b).

By applying the Ampere's circuital law, the magnetic flux equation and the reluctance equations, the magnetic circuit can be presented as the following:

$$H_m L_m + B_g A_g R_g = NI \quad (3)$$

$$B_m A_m = B_g A_g (R_g / R_T) \quad (4)$$

$$R_g = g_0 / (\mu_0 A_g) \quad (5)$$

$$R_m = L_m / (\mu_0 \mu_r A_m) \quad (6)$$

From equation (1), (3), (4) and (6), the operating flux density of the magnet can be written as

$$B_m = (B_r R_m + NI / A_m) / (R_m + R_T) \quad (7)$$

The operating flux density has been changed due to the magnetizing force from the EM coils. Figure 3 illustrates the load line of the magnet shifted parallel from its original load line. For the PM/EM bearing, the magnet will mainly operate at near zero magnetizing force so the operating flux density can be treated as a constant value of B_m with a variation ΔB_m . Furthermore, the permanent magnet design and the EM coil design can be studied independently as long as the

operating point of the magnet is along the straight line of the B-H curve. Equation (7) can be rewritten as the following:

$$B_m = B_r R_m / (R_m + R_T) \quad (8)$$

$$\Delta B_m = (NI/A_m) / (R_m + R_T) \quad (9)$$

In the PM/EM bearing the magnetic flux from one permanent magnet passes the one air gap to the return ring of the flywheel and return through the other air gap. The equation for the reluctance of the air gap is doubled,

$$R_g = 2g_o / \mu_o A_g \quad (10)$$

The bias flux generated by the permanent magnet is

$$B_u = (B_m A_m / A_g) (R_T / R_g) \quad (11)$$

The permanent magnet design is statically undetermined because there are five equations: (1), (6), (8), (10) and (11) with 12 variables: B_m , B_r , B_u , H_m , μ_r , L_m , g_o , A_m , A_g , R_T , R_m and R_g .

In the magnetic bearing design there are four EM coils of the same axis connected in parallel to the power amplifier. The magnetomotive force of the EM coils in each axis is NI_{max} . The flux density generated by the EM coils across the air gap is

$$B_{EM} = \mu_o NI_{max} / (4g_o) \quad (12)$$

STIFFNESS MODEL

The stiffness model for the magnetic bearing assumes the properties of the bearing to be linear over the operating range except the control current to the EM coils in the control system. The control current is linear until saturation of the power amplifier, after which it is held constant. The reason for the limitation of the control current is to avoid a magnetic saturation of the materials.

The static behavior of the bearing can be represented by force equilibrium equations. In the axial direction, the bearing passively supports the axial load of the flywheel.

$$F_A = K_z d_p \quad (13)$$

In the radial direction, the flywheel is affected by two forces: the destabilizing force from permanent magnets and the corrective force from electromagnetic coils. The combined restoring force of the bearing is

$$F_{rad} = K_i I - K_x X \quad (14)$$

Figure 5(a) represents the radial forces of the bearing including the destabilizing force, the corrective force, and the restoring force. Figure 5(b) shows the control current output from the power amplifier. The corrective force reaches its peak when the power amplifier becomes saturated and cannot supply more current. Simultaneously the restoring force also reaches the peak and begins to decline as the destabilizing force continues to increase and the corrective force stays constant. When the net restoring force is zero, the corrective force equals the destabilizing force. The maximum displacement of flywheel is defined as the maximum stable range and given by

$$X_{stb} = K_i I_{max} / K_x \quad (15)$$

There is a maximum displacement range the flywheel can travel without current saturation. The maximum range X_{lin} is called the linear range of the bearing, which is dependent on the current/displacement ratio C of the control system.

$$X_{lin} = I_{max} / C. \quad (16)$$

In the linear range, the force equilibrium equation (14) can also be written as

$$F_{rad} = K_a X = K_i I - K_x X \quad (17)$$

This active stiffness of bearing can be represented by

$$K_a = C K_i - K_x \quad (18)$$

The linear range, the maximum restoring force and the active stiffness are determined not only by the maximum control current to the EM coils but by the current/displacement ratio C of the control system. A lower current/displacement ratio means a larger linear range, lower active stiffness and smaller maximum restoring force. A higher current/displacement ratio has the opposite effects. For a magnetic bearing, a larger linear range, higher active stiffness and greater maximum restoring force are desired so there is a conflicting interest for the choice of the C . The bearing must balance all these performance requirements.

The geometric dimensions of the bearing such as the length and the cross section area of the air gap have major effects on the magnetic flux and the magnetic force because the flux directly across the air gap of two pole faces helps to support the weight as well as center the flywheel. The bias flux from the permanent magnet contributes the axial stiffness K_z and the passive radial stiffness K_x . The flux from both the permanent magnet and EM coils influences the force/current sensitivity K_i . The K_z , K_x and K_i values can be obtained from experimental or a theoretical analysis.

The axial stiffness of the magnetic bearing derived by Sabnis [4] using the Schwartz-Christoffel transformation shows that

$$K_z = 4B_u^2 R_{mean} / \mu_0 \quad (19)$$

The passive radial stiffness and the force/current sensitivity can be derived as the following [1]:

$$K_x = 2p B_u^2 R_{mean} t p f / (\mu_0 g_0) \quad (20)$$

$$K_i = 2B_u R_{mean} t p f N / g_0 \quad (21)$$

PERMANENT MAGNET DESIGN

Permanent magnetic materials have greatly progressed in last decade due to the development of rare earth magnets [5]. Rare earth magnets such as samarium-cobalt and neodymium-iron-boron magnets have very high coercive forces combining with high remanence. Figure 6 shows the B-H curves of the rare-earth magnets compared to some older magnet types such as Alnico and ceramic magnets. The B-H curves for the rare-earth magnets are nearly straight lines in most of the second quadrant. The energy products of the rare earth magnet are four or five times values of older magnet types. It means smaller magnets can now generate same magnetic flux. A straight B-H curve also means the recoil lines of minor hysteresis loops will closely follow the B-H curve. The magnets can handle the external magnetizing force and any variation of the air gap in the magnetic circuit without degrading the performance. Thus, the rare earth magnets induce an easier magnetic circuit design with more dynamic applications.

Although there are many rare earth magnets, the commercially available magnets are generally separated into three groups: $SmCo_5$, Sm_2Co_{17} , and $NdFeB$. $SmCo_5$ magnets are the first type of rare earth magnets and produce an energy product of 16 to 23 MGOe with very high intrinsic coercive force, which can resist strong adverse magnetizing fields. They have a high curie temperature at $750^\circ C$ but the intrinsic coercive force drops off as the temperature increases. $SmCo_5$ magnets can only be used to about $250^\circ C$. Sm_2Co_{17} magnets have a higher energy product of 20 to 30 MGOe and a higher remanence of 9.5 to 12 KG. Some types of Sm_2Co_{17} have a lower intrinsic coercive force that results in a knee in the B-H curve. Sm_2Co_{17} magnets have slightly better temperature performance than $SmCo_5$ and are useful to about $350^\circ C$. $NdFeB$ magnets have the highest energy product of 25 to 40 MGOe and a remanence of 11 to 12.8 KG. $NdFeB$

magnets only have a curie temperature of 300°C and are useful only below 150°C. NdFeB is the cheapest rare earth component due to the vast amounts of the material resources currently available. NdFeB has a corrosion problem, however, and Sm_xCo_x magnets should not be used at the radiation environments. All three magnets are very hard and brittle and should be protected from large mechanical stresses.

The PM design has 5 equations with 12 variables as suggested from the reluctance model. Three dependent variables H_m, R_m and R_g can be eliminated using equations (1), (6) and (10). Three variable B_u, A_g and g_o are determined by the axial drop, axial load and radial load requirements. If the fundamental geometry of the magnetic circuit is known, the useful flux ratio (R_T/R_g) is approximated. For the current PM/EM bearing design, the useful flux ratio is in the range of 30% to 40%. The relative recoil permeability μ_r for the rare earth magnets is around 1.05. The PM design problem has been simplified into 2 equations, (8) and (11), with 4 variables: B_m, B_r, L_m and A_m.

For a maximum energy output from the permanent magnet, the operating flux density should be half its remanence. This design can also minimize the volume of the magnet and its material cost, and equates to

$$B_m = B_r/2 \text{ or } R_m = R_T \quad (22)$$

This may not be feasible due to other geometric constraints on the length and cross section area of the magnet. To avoid underestimation of the reluctance in the magnetic circuit or increase of the air gap, the operating flux density B_m is always designed above its calculated value (half the remanence). However, the B_m/B_r ratio is a good efficiency index for the magnet design. This B_m/B_r ratio can be used to choose an appropriate permanent magnet strength form the manufacturer catalog at a preliminary design.

Any two of the five variables: B_m, B_r, L_m, A_m and B_m/B_r can be chosen to solve the following equations derived from Equation (8) and (11),

$$B_r = (B_u A_g / A_m) (R_g / R_T) (B_r / B_m) \quad (23)$$

$$L_m / A_m = (\mu_r g_o / A_g) (R_T / R_g) / ((B_r / B_m) - 1) \quad (24)$$

$$A_m = B_g A_g L_m (R_g / R_T) / (B_r L_m - \mu_r B_g g_o) \quad (25)$$

PM design is one of the most difficult in the magnetic bearing because all the magnetic flux paths should be carefully calculated. The rare earth magnets are expensive and usually made to order for a specific configuration. If there is error in the design, the magnets most likely will be wasted.

ELECTROMAGNETIC COIL DESIGN

The EM coil design is based on the stability and the force slew rate considerations to choose the number of turns for the coil, and the voltage and current for the power amplifier. The stability consideration is derived from the nonlinear control system analysis used to remove the limit cycle oscillation and to improve the robustness of the bearing. The force slew rate consideration is derived from the dynamics requirements of the magnetic bearing for the external force or mass unbalance conditions. From both the experimental results and theoretical analysis the power amplifier voltage and the number of turns (inductance) of the EM coils have greater roles in stabilizing the bearing and responding to any disturbance.

Zmood et al [6] found, when the power was connected, the flywheel not only failed to self-suspend but often broke into self-sustaining oscillation unless the mechanical touchdown gap was well adjusted. Also, the magnetic bearing flywheel system broke into limit cycle oscillation due to a

large disturbance. The source of the oscillations is due to the combined effects of the power amplifier saturation, bearing radial stiffness K_x , the touchdown gap X_{td} and the inductance of the EM coil. A simplified nonlinear control system model shown in Figure 7 has been built to study the self-suspension and limit cycle oscillation phenomenon observed in the experiment. The model makes the following assumptions:

- (1) The back e.m.f. induced in the EM coils can be neglected;
- (2) The EM coil resistance can be neglected;
- (3) When the flywheel collides with the touchdown bearing the velocity and acceleration drop to zero;
- (4) There is no external disturbance force so the equation (14) can be applied;
- (5) There are only the current and displacement feedback loops;
- (6) The bearing actuator can be approximately modelled by a first order differential equation.

The equation for the stability condition of the bearing can be written as the following

$$1 < \frac{K_i C_x}{K_x C_i} < \frac{1}{2} + \sqrt{\frac{1}{4} + \frac{K_i \alpha'}{K_x X_{td}}} \quad (26)$$

where $\alpha' = V_{cc}/(W_m' L_{ind})$ and $W_m' = (K_x/M)^{1/2}$.

For a stable system the parameters of the control system, C_x and C_i , should be chosen to satisfy the inequality equation (26). To increase the robustness of the control system and to relax the restriction on these parameters the right hand part of the inequality equation should be as large as possible. This part can also be viewed as the relative stability ratio δ of the control system. For our magnetic bearing there are four EM coils connected parallel together to the power amplifier at one axis. The magnetic flux from the EM coils will pass four air gap so the inductance becomes

$$L_{ind} = \mu_0 A_g N^2 / (4g_0) \quad (27)$$

From equation (26) and (27) the number of turns for the EM coil can be written as an inequality form.

$$N < \frac{4\sqrt{2}g_0}{\pi^2 B_u R_{meantpf}} \frac{V_{cc}}{W_m' X_{td}} \frac{1}{\delta^2 - \delta} \quad (28)$$

Maslen et al [7] studied the effects of the force slew rate on the dynamic performance of the bearing. If the bearing operates about its center, $X = 0$, the force slew rate can be derived from the radial force equation (14) as

$$dF/dt = K_i(dI/dt) \quad (29)$$

The force slew rate can also be written as the function of the applied voltage and the inductance of the EM coils.

$$dF/dt = K_i V_{cc} / L_{ind} \quad (30)$$

For a step force input F_R or a mass unbalance at a rotational speed of w rad/s with a distance X from the center, the force slew rate is proven to be

$$dF/dt > (2F_R^3 / 3MX)^{1/2} \quad (31)$$

$$dF/dt > Mw^3 X \quad (32)$$

The number of turns for the EM coils presented as the function of the force slew rate becomes

$$N < \frac{8\sqrt{2}B_u V_{cc}}{\pi\mu_0 \frac{dF}{dt}} \quad (33)$$

The maximum supply current for the EM coils can be calculated using equation (12),

$$I_{\max} = 4B_{EM}g_0/\mu_0N \quad (34)$$

The power amplifier of the control system can be chosen based on the its voltage and current requirements.

PM/EM MAGNETIC BEARING DESIGN

The flowchart for the design methodology of the PM/EM bearing is shown in Figure 8. The design procedures start with design requirements for the magnetic bearing including the mass of the flywheel, the axial force, the radial force and the linear operating range. There are some initial inputs such as the saturation flux density of the magnetic material, the recoil permeability of the PM material, the operating point of the permanent magnet, the useful flux ratio, and power amplifier voltage. These values can be updated or changed with the choice of the specific materials and designs.

The bearing design is an iterative processes so the number of steps just shows a possible sequence. These procedures are used for the magnetic bearing flywheel energy storage system and designer can revise the procedures for other applications.

(1) Flux density consideration

The flux densities in any section of the magnetic bearing are limited by the saturation value of the magnetic material so the combined flux densities from the PM and EM are less than the saturation value. If there are equal flux densities from the PM and EM, the bearing can generate a maximum force. In most applications the flux density from the PM is greater than that from the EM.

(2) Geometric relationship consideration

Our PM/EM bearing is a small gap suspension design so the linear range is less than 15% of the air gap. To avoid large leakage flux and cross-talk between the pole faces of the magnet plates and return ring, the pole face thickness is at least 3 times of the air gap. Also, there is a minimum thickness for the PM to prevent too much leakage between the two magnet plates.

(3) Axial drop, axial load, and radial force consideration

The magnetic bearing is designed to satisfy the force requirements by choosing the flux densities and the geometric dimensions. Because of our radial active bearing design the load capability in the axial direction is weaker than the radial direction. If the bearing is used to handle the same force in both directions, the axial force requirement becomes dominate. To avoid the possibility that a larger axial drop may worsen the magnetic properties of the bearing the ratio of the axial drop and the pole face thickness is limited to 20%.

(4) Selection of a feasible design

After satisfying the performance requirement and physical constraints a feasible design is chosen including the flux densities from the PM and EM, the mean radius, the air gap, the pole face thickness, and other dimensions.

(5) Permanent magnet design

Using the information from the previous step the parameters of the permanent magnet design such as the magnet strength, thickness and cross section area can be decided by applying the equation (23), (24) and (25).

(6) Electromagnetic coil design

Based on the stability and force slew rate considerations the number of turns for the EM coils as well as the voltage and current for the power amplifier can be decided.

(7) Characteristics of the PM/EM bearing

The performance parameters such as X_{stb} , X_{lin} , K_a , C , K_z , K_x and K_i for the bearing can be calculated using the equation (15), (16), (17), (18), (19), (20) and (21).

(8) Optimization design

An optimization method for the PM/EM bearing design has been developed at the University of Maryland [8]. The designer can define an objective function with all equality and inequality constraints to find an optimum design.

After finishing the preliminary design the bearing needs a detailed study such as a finite element model for magnetic circuit agreement and dynamic simulation. Also, the control system and overall bearing flywheel system need further investigation but these are beyond the scope of this paper.

EXAMPLE

An example for the pancake magnetic bearing design is presented to demonstrate the proposed design methodology. Assume a pancake magnetic bearing for the energy storage system having a flywheel weight of 8 lbs. The bearing is designed to handle at least 16 lbs force at both axial and radial direction with an axial drop of no more than 20% of its pole face thickness. The magnetic bearing should allow at least 0.006 inch for the radial displacement before being limited by the mechanical touchdown bearing. The magnetic material for the bearing is nickel iron which has a saturation flux density of 1 Tesla. The maximum radius for the bearing is limited to 2 inch and the minimum height of the permanent magnet is 0.3 inch. The power amplifier of the control system has a voltage 24 volts and a maximum supply current 1.5 Ampere. The useful flux ratio is assumed to be 40% for this design.

(1) Design Requirements & Physical Constraints

The performance requirement and physical constraints of the magnetic bearing are rewritten as the following:

$$M = 8 \text{ lbs}$$

$$F_A \geq 16 \text{ lbs}$$

$$F_R \geq 16 \text{ lbs}$$

$$B_{sat} = 1 \text{ Tesla}$$

$$R_{mean} \leq 2 \text{ in}$$

$$X_{td} = 0.006 \text{ inch}$$

$$dp/tpf \leq 0.2$$

$$L_m \geq 0.3 \text{ inch}$$

$$V_{cc} = 24 \text{ V}$$

$$I_{max} \leq 1.5 \text{ Amp}$$

$$R_T/R_g = 0.4$$

(2) Flux Density Consideration

The flux density generated by the permanent magnet across the air gap is assumed to be 50% of the saturation value of magnetic material. The flux density from the EM coils is 40% of the saturation value.

$$B_u = 0.5 B_{sat} = 0.5 \text{ Tesla}$$

$$B_{EM} = 0.4 B_{sat} = 0.4 \text{ Tesla}$$

(3) Geometric Relationship

The touchdown gap is designed to be 15% of the air gap and the pole face thickness is three time of the air gap.

$$g_o = X_{td}/0.15 = 0.04 \text{ in}$$

$$tpf = 3 g_0 = 0.12 \text{ in}$$

(4) Axial Drop, Axial Load and Radial Force Requirement

The axial stiffness equation is used to find the mean radius for the magnetic bearing.

$$d_p = W_A/K_z = 0.2 \text{ tpf} = 0.024 \text{ in}$$

$$R_{\text{mean}} = 2.89 \text{ in} > 2 \text{ in (Failure!)}$$

Because the calculated radius is larger than the allowable size the above design must be changed. One way is to choose the bearing radius as the maximum allowable value and to find the required flux density at the air gap which can satisfy the requirement.

$$R_{\text{mean}} = 2 \text{ in}$$

$$B_u = 0.6 \text{ Tesla}$$

$$B_{EM} = 0.3 \text{ Tesla}$$

$$F_A = 20.9 \text{ lbs} > 16 \text{ lbs (OK!)}$$

$$F_R = 25.1 \text{ lb} > 16 \text{ lbs (OK!)}$$

(5) Permanent Magnet Design

The permanent magnet is chosen to use the rare earth Recoma 20 material which has a remanence of 0.85 Tesla and a recoil permeability of 1.05. The length of the permanent magnet is assumed to be 0.3 in. The cross section area for the air gap is calculated to be 0.377 in². The radius and the operating flux density of the magnet can be calculated as the below

$$A_m = 0.829 \text{ in}^2$$

$$R_m = 0.94 \text{ in}$$

$$B_m = 0.68 \text{ Tesla}$$

(6) Electromagnetic Coil Design

The radial passive stiffness of the bearing is calculated to be 1567 lb/in. If the relative stability ratio is assumed to be 2, the number of turns for the EM coil can be calculated using the stability criteria

$$N < 1790 \text{ turns}$$

If the bearing is assumed to handle a step input force of 16 lbs at the touchdown gap. The force slew rate and the number of turns for the coil are:

$$dF/dt = 31254 \text{ N/s}$$

$$N < 1320 \text{ turns}$$

Finally the number of turns for the EM coil is chosen to be 1000 turns so the maximum supply current is 0.97 ampere which satisfies the constraint of the power amplifier.

(7) Characteristics of Pancake Magnetic Bearing

The performance parameters for the bearing are listed as the following:

$$K_x = 1567 \text{ lb/in}$$

$$K_i = 29.1 \text{ lb/Amp}$$

$$K_a = 2667 \text{ lb/in}$$

$$K_z = 332 \text{ lb/in}$$

$$C = 146 \text{ Amp/in}$$

$$X_{\text{stb}} = 0.018 \text{ in}$$

$$X_{\text{lin}} = 0.0066 \text{ in}$$

DISCUSSION AND CONCLUSION

In light of the demands of modern technology for more efficient and economic energy conversion, magnetic bearings certainly fit the requirements. The various magnetic bearings differ in function and form but a major commonality between them should be the theory that governs all physical and magnetic behavior. Although the specific numbers of these mathematical models for a flywheel

magnetic bearing are unique, the design methodology and magnetic developments encompass all such devices. As always, one must be careful to study the physical constraints and boundary conditions placed on the problem. University of Maryland has been successful in developing two different sizes of bearings and an operational combination of two bearings in a stack configuration. The success has come from proposing, modifying, and verifying the mathematical models presented here. A few grey areas remain, such as the crosstalk between magnetic flux paths and harmonic disturbances, which were beyond the scope of this paper. Future methodology will include dynamic effects, digital rather than analog control, and finite element analysis of the magnetic circuitry. As the system becomes more complex, so do the questions that are raised about its optimization.

SYMBOLS AND ABBREVIATIONS

Ag:	Cross Section Area of Air Gap; for PM/EM Bearing = $\pi R_{mean} t_p / 2$
Am:	Cross Section Area of Permanent Magnet = $\pi D_m^2 / 4$
BEM:	Flux Density by Electromagnet at Pole Face
Bm:	Operating Flux Density of Permanent Magnet
Br:	Remanence of Permanent Magnet
Bsat:	Saturation Value of Magnetic Material
Bu:	Useful Flux Density by Permanent Magnet at Pole Face
Bg:	Flux Density Across Air Gap
C:	Current/Displacement Ratio of Control System
Cx:	Displacement Feedback Gain in Control System
Ci:	Current Feedback Gain in Control System
Dm:	Diameter of Permanent Magnet
dp:	Axial Drop of Flywheel
FA:	Maximum Axial Force
FR:	Maximum Radial Force at $X = X_{td}$
Frad:	Restoring Radial Force = $K_{il} - K_x X$
go:	Air Gap
Hc:	Coercive Force of Permanent Magnet
Hm:	Magnetizing Force of Permanent Magnet
Imax:	Maximum Control Current to Electromagnetic Coils
Ka:	Active Stiffness of Magnetic Bearing = $CK_i - K_x$
Ki:	Force/Current Sensitivity of Electromagnetic Coils
Kx:	Passive Radial Stiffness of Magnetic Bearing
Kz:	Passive Axial Stiffness of Magnetic Bearing
Lind:	Inductance of Electromagnetic Coils
Lm:	Length of Permanent Magnet
M:	Mass of Flywheel
N:	Number of Turns of One Electromagnetic Coils
Rg:	Reluctance of Air Gap at Pole Face
RL:	Reluctance of Leakage Flux
Rm:	Reluctance of Permanent Magnet
RT:	Total Reluctance = $R_g R_L / (R_g + R_L)$
Rmean:	Mean Radius of Middle Point of Air Gap
tpf:	Pole Face Thickness
Xlin:	Linear Range of Magnetic Bearing
Xstb:	Stable Range of Magnetic Bearing = $X_{lin} (1 + K_a / K_x)$
Xtd:	Touchdown Gap
Vcc:	Amplifier Supply Voltage
μ_0 :	Permeability of Free Space = $4\pi \times 10^{-7}$ H/m
μ_r :	Recoil Permeability of Permanent Magnet

$\frac{dF}{dt}$: Force Slew Rate

ΔB_m : Varying Flux Density of Permanent Magnet

REFERENCE

1. Iwaskiw, A. P., "Design of a 500WH Magnetically Suspended Flywheel Energy Storage System", Master Thesis, University of Maryland, College Park, 1987.
2. McCaig, M., Clegg A. G., "Permanent Magnets in Theory and Practice", John Wiley & Sons, Inc., New York, 1987.
3. Parker, R. J., "Advances in Permanent Magnetism", John Wiley & Sons, Inc., New York, 1990.
4. Sabnis, A. V., "Analytical Techniques for Magnetic Bearings" PhD Dissertation, Univ. of California, Berkeley, 1974.
5. Strnat, K. J., "Modern Permanent Magnets for Applications in Electro-Technology", Proceedings of International Workshops on Rare-Earth Permanent Magnets and Applications, Pittsburgh, Penn., 1990.
6. Zmood, R. B., Pang D., Anand D. K., Kirk, J. A., "Improved Operation of Magnetic Bearings for Flywheel Energy Storage System", Proceedings of 25th Intersociety Energy Conversion Engineering Conference, Reno, Nevada, 1990.
7. Maslen, E., Hermann, P., Scott, M., Humphris, R. R., "Practical Limits to the Performance of Magnetic Bearings: Peak Force, Slew Rate, and Displacement Sensitivity", Proceedings of NASA Workshop on Magnetic Bearings, Langley, Virginia, 1988.
8. Pang, D., Kirk, J. A., Anand, D. K., Huang, C., "Design Optimization for Magnetic Bearing", Proceedings of 26th Intersociety Energy Conversion Engineering Conference, Boston, Mass., 1991.

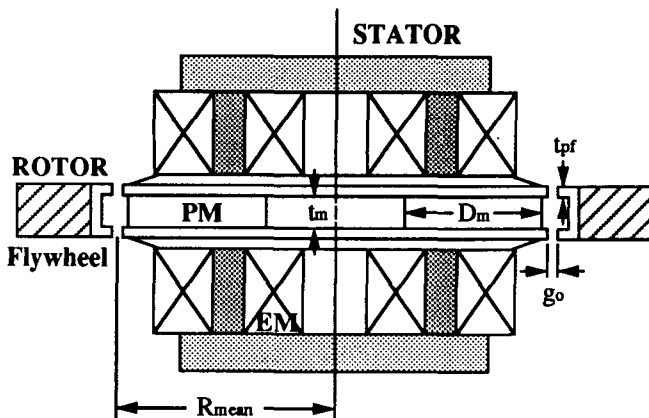


Fig. 1 PM/EM Magnetic Bearing

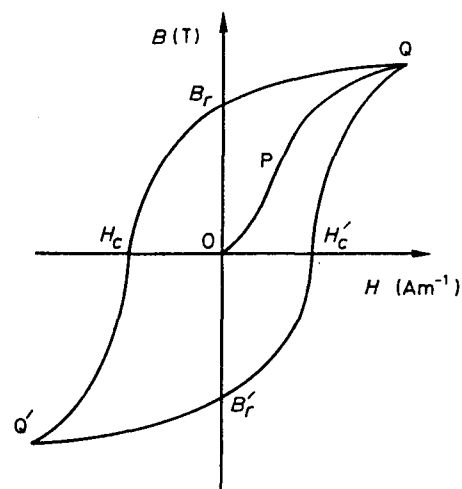


Fig. 2 PM Hysteresis Loop

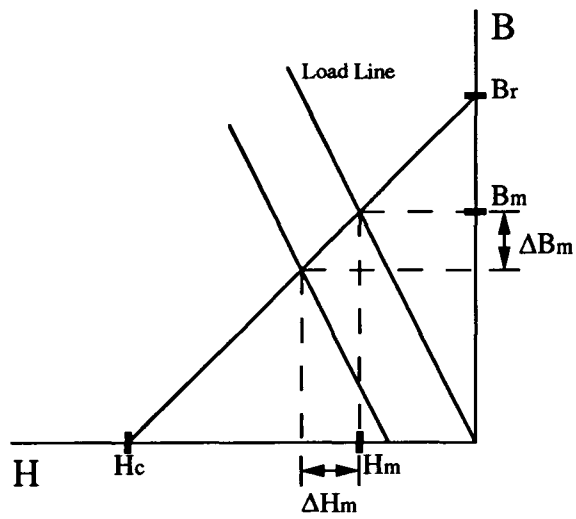


Fig. 3 Ideal PM B-H Curve

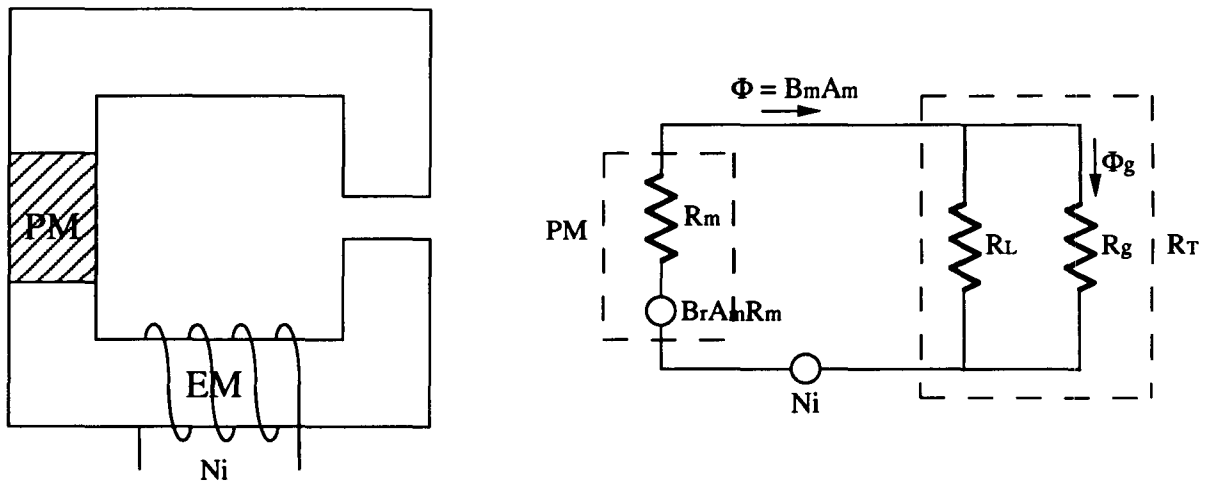


Fig. 4 PM/EM Magnetic Circuit

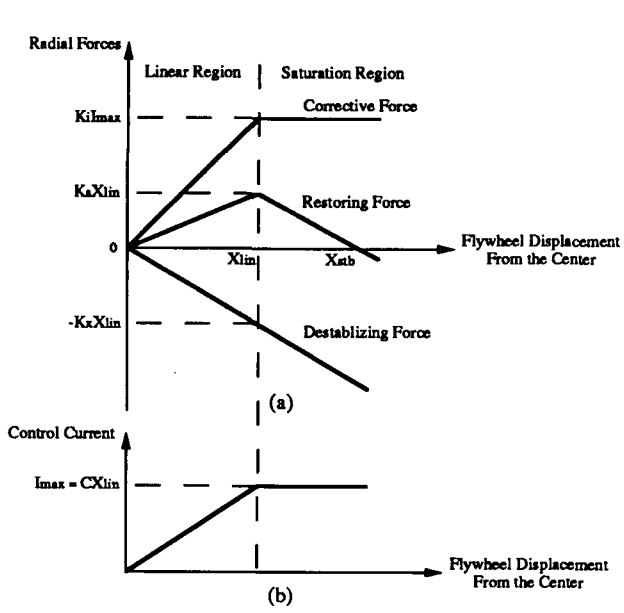


Fig. 5 Magnetic Bearing Radial Forces

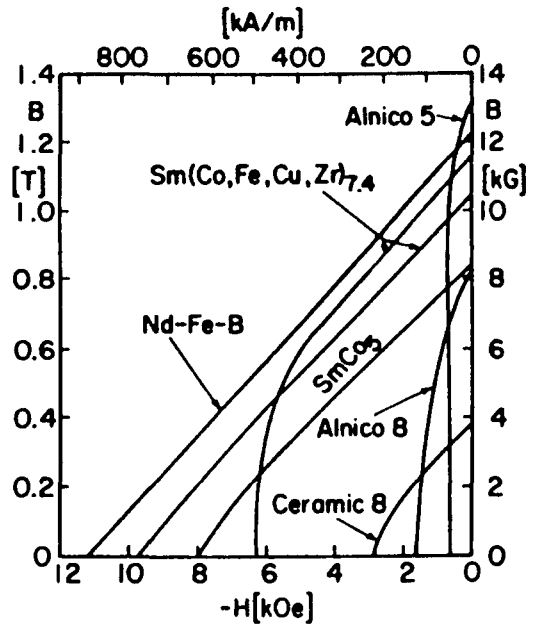


Fig. 6 Various PM B-H Curves

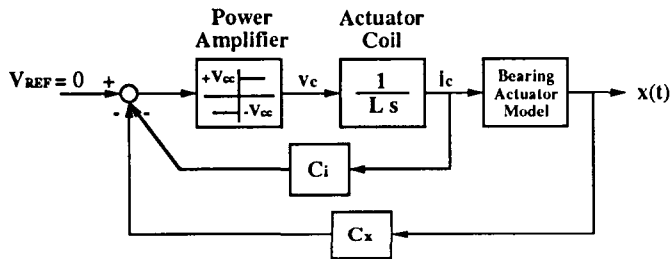


Fig. 7 Simplified Bearing Control System

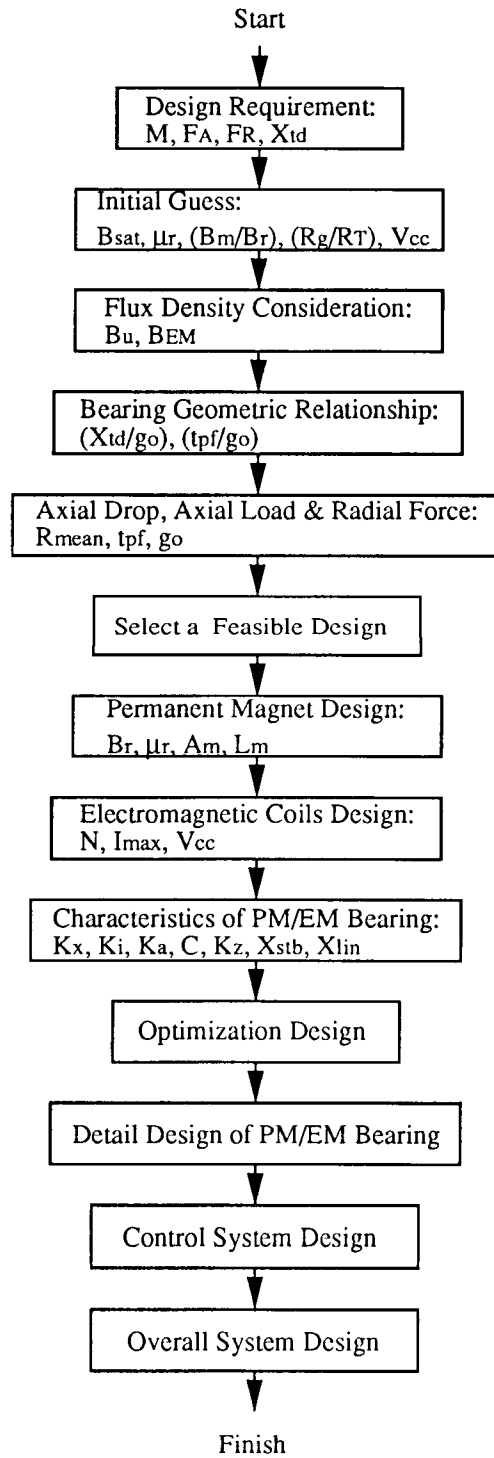


Fig. 8 PM/EM Bearing Design Flowchart